Journal of ELECTRONIC MATERIALS, Vol. 46, No. 1, 2017
DOI: 10.1007/s11664-016-4916-4

Dielectric Properties of Reduced Graphene Oxide/Copper Phthalocyanine Nanocomposites Fabricated Through π–π Interaction

ZICHENG WANG,[1] RENBO WEI ,[1,2] and XIAOBO LIU[1,3]

1.—Research Branch of Advanced Functional Materials, School of Microelectronics and Solid-State Electronics, High Temperature Resistant Polymer and Composites Key Laboratory of Sichuan Province, University of Electronic Science and Technology of China, Chengdu 610054, China. 2.—e-mail: weirb10@uestc.edu.cn. 3.—e-mail: liuxb@uestc.edu.cn

Reduced graphene oxide/copper phthalocyanine nanocomposites are successfully prepared through a simple and effective two-step method, involving preferential reduction of graphene oxide and followed by self-assembly with copper phthalocyanine. The results of photographs, ultraviolet visible, x-ray diffraction, x-ray photoelectron spectroscopy, and scanning electron microscopy show that the *in situ* blending method can effectively facilitate graphene sheets to disperse homogenously in the copper phthalocyanine matrix through π–π interactions. As a result, the reduction of graphene oxide and restoration of the sp^2 carbon sites in graphene can enhance the dielectric properties and alternating current conductivity of copper phthalocyanine effectively.

Key words: Dielectric properties, copper phthalocyanine, reduced graphene oxide, *in situ* blending method, nanocomposites

INTRODUCTION

Graphene, a two-dimensional (2D) sheet of sp^2-hybridized carbon arranged in a honeycomb lattice, has received increasing attention due to its outstanding electrical, thermal, mechanical, and optical properties,[1–4] which offer a wide range of potential applications, such as energy storage, sensors, supercapacitors, and catalysts.[5–8] However, due to the strong π–π stacking tendency and high cohesive energy, pure graphene tends to agglomerate or restack easily,[9] which greatly hinders its further application. Therefore, modification on the surface of graphene is a widely adopted method. At present, the most common approach to modify graphene is the using of strong oxidizing agents to exfoliate pristine graphite.[10–13] The obtained contiguous aromatic lattice of graphene is simultaneously interrupted by epoxide, hydroxy, and carboxylic groups,[14,15] offering graphene oxide (GO). Comparing with pure graphene, the introduction of the hydrophilic oxygenic groups on the basal plane and edge of GO can improve the dispersion and adhesion of graphene sheets in solvents and/or matrices effectively. Meanwhile, the obtained GO possesses a similar anisotropic nature and comparable mechanical strength with graphene[16] and can be easily reduced back to graphene with excellent electrical conductivity.[17,18] Therefore, GO, as a very important precursor of graphene, has been employed as an excellent additive for improving the physical performance of resin materials.[19,20]

Copper phthalocyanine (CuPc) and phthalocyanine derivatives have attracted considerable interest owing to their fascinating properties and potential applications.[21,22] Making use of the aromatic heterocyclic molecules with high symmetry, planarity, and 18 π-electron delocalized systems, the applications including serving as building block for fabricating solar cell, fuel cells, optical-limiting materials, gas sensors, and field-effect transistors[23–26] have been actively explored. Among these applications, the dielectric property is one of the most important parameters. However, the relatively

Zicheng Wang and Renbo Wei contribute equally to this work.
(Received May 18, 2016; accepted August 25, 2016; published online September 9, 2016)

low intrinsic dielectric constant (~4) of CuPc restricts its further application, which needs to be improved urgently.[27] In our previous study,[28] we prepared a CuPc composite with a dielectric constant as high as 164.8 at 1 kHz by self-assembly in the orientationally ordered liquid crystalline state of GO. According to the Maxwell–Wagner–Sillars (MWS) interfacial polarization theory,[29] the dielectric constant of the CuPc composite can be further improved if graphene and/or reduced graphene oxide (RGO), whose conductivity is much better than that of GO, is used.

GO, as a very important precursor of graphene, has a large 2D planar structure which is consisted of two parts: oxygen-functional groups and graphitic domain. The graphitic domain is mainly composed of sp^2 carbon. The delocalized π-electron system of graphitic domain effectively facilitates interaction with CuPc through the strong π–π stacking interaction. Unfortunately, the oxygen-functional groups of GO, especially the carboxyl and epoxy species, tend to act as a ligand that coordinates with the central copper ions of CuPc.[30] The formation of the metal–ligand coordination bond will strengthen the stability of oxygen-functional groups, which hinders their breakaway during the process of GO reduction. As a result, it is difficult to restore the electrical conductivity of graphene. Hence, in this paper, we report a facile and effective approach to prepare reduced graphene oxide/copper phthalocyanine (RGO/CuPc) nanocomposites with high dielectric properties by preferential reduction of graphene oxide, which was used as a template for the self-assembly of CuPc through π–π interactions between graphene sheets and Pc rings of CuPc. The preparation and dielectric properties of the RGO/CuPc nanocomposites are studied in detail.

EXPERIMENTAL

Materials

Graphene oxide (GO) was purchased from XFNANO Materials Tech Co. Ltd (Nanjing, China). 4,4′-bis(3,4-dicyanophenoxy)biphenyl (BPH) was synthesized in our laboratory by the previously reported method.[31] Cuprous chloride (CuCl), *N*,*N*-dimethylformamide (DMF) and *N*,*N*-dimethylacetamide (DMAc) were purchased from by Tianjin BODI chemicals, Tianjin, China. Hydrazine monohydrate (98%) was purchased from Sigma Aldrich. All other reagents were commercially available products and used as received without further purification.

Preparation of Copper Phthalocyanine (CuPc)

A 1.31-g (3 mmol) sample of BPH and 0.10 g (1 mmol) CuCl were dissolved in 40 mL of DMAc and stirred at 160°C for 4 h. After that, the solution was cooled down to room temperature. The crude product was collected by filtration, washed with water, and dried in vacuum. After refluxing in methanol twice, the product was filtrated and washed with cold methanol for three times. The blue powdery product was dried in vacuum at 50°C for 24 h. Yield: 70%.

Reduction of Graphene Oxide by Hydrazine Monohydrate

GO (25 mg) was added in a 250 mL round bottom flask and a 80-mL solvent mixture of H_2O and DMF (volume ratio DMF: H_2O = 9:1) was added slowly, the system was vigorously stirred and sonicated for 1 h, yielding a homogeneous dispersion of the graphene oxide sheets. Hydrazine monohydrate (8 μL) was subsequently added to the dispersions. After being stirred with a Teflon-coated stirring bar at 80°C for 12 h, the mixture was cooled down to room temperature, yielding black dispersions of RGO sheets. In order to investigate the conversion from GO to RGO, the reaction time was varied from 0 to 12 h. The corresponding products were denoted as GO, RGO-4h, RGO-8h, and RGO-12h.

Preparation of Reduced Graphene Oxide/Copper Phthalocyanine (RGO/CuPc) Nanocomposites

CuPc (0.48 g) was dissolved in DMF (20 mL), then the obtained solution was dropped into the RGO suspension (W_{CuPc}:W_{GO} = 95:5) with vigorous mechanical stirring for 2 h. After adding into 200 mL of water, the crude product was collected by filtration. The product was purified by washing with 300 mL water three times and then dried at 80°C for 24 h in vacuum. The other products with the same content of GO (5 wt.%) were obtained by using the similar procedure and conditions, and denoted as GO/CuPc, RGO-4h/CuPc, RGO-8h/CuPc, and RGO-12h/CuPc (5RGO/CuPc), respectively. In addition, samples with 10 wt.% (10RGO/CuPc), 15 wt.% (15RGO/CuPc) of GO that was reduced for 12 h were also prepared.

Characterization

Ultraviolet visible (UV–Vis) absorption spectra were obtained on a UV2501-PC spectrophotometer. Differential scanning calorimetry (DSC) analysis was carried out using a TA Q100 system under nitrogen atmosphere at a heating rate of 10°C/min. X-ray diffraction (XRD) patterns were recorded on a Rigaku RINT 2400 with Cu Kα radiation. Scanning electron microscopy (SEM) images were taken on a JSM 6490LV (JEOL, Japan) field emission microscope. X-ray photoelectron spectroscopic (XPS) measurements were carried out on an ESCA 2000 (VG Microtech, UK) using a monochromic Al Kα ($h\nu$ = 1486.6 eV) x-ray source. Dielectric measurements were carried out by using an Agilent 4284A dielectric analyzer.

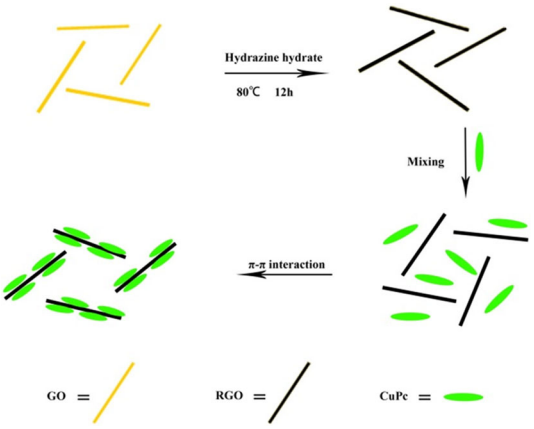

Scheme 1. The synthetic route of RGO/CuPc nanocomposites.

RESULTS AND DISCUSSION

In this study, reduced graphene oxide/copper phthalocyanine (RGO/CuPc) nanocomposites were fabricated, as shown in Scheme 1. Firstly, RGO was prepared by reducing GO with hydrazine monohydrate. Secondly, RGO dispersions were homogeneously mixed with CuPc. Through π–π interaction between the RGO and CuPc, RGO/CuPc nanocomposites were obtained after the self-assembly between them.

Reduction of Graphene Oxide

Figure 1 shows the photographs of GO dispersions with concentration of 0.1 mg/mL in the mixture solvent H_2O/DMF (1:9) before and after reduction by hydrazine monohydrate for different time. As shown in Fig. 1a, the dispersions of GO is homogeneous and bright yellow–brown in color. After reduced by hydrazine monohydrate, the color of the dispersion transfers to black gradually, indicating the efficiency of the reduction of GO. More importantly, the obtained RGO can be homogeneously dispersed in the mixture solvent (H_2O/DMF) and is stable for several weeks, which provides a favorable precondition for uniformly blending with CuPc.

UV–Vis Spectra of RGOs in Water

In ordered to monitor the reduction process of GO, time-dependent UV–Vis spectra were recorded, as shown in Fig. 2. The UV–Vis spectrum of GO dispersed in water exhibits two characteristic peaks: an absorption peak centered at 227 nm, corresponding to $\pi \rightarrow \pi^*$ transitions of aromatic C=C bonds and a shoulder peak at ~301 nm, which can be assigned to $n \rightarrow \pi^*$ transitions of C=O bonds.[32] After the reduction by hydrazine monohydrate, the absorption peak of C=C bonds red-shifts to 235 nm, 273 nm and 274 nm gradually with the increasing of the reduction time from 4 h, 8 h, and 12 h. This is mainly attributed to the restoration of the π-conjugated network within the graphene and

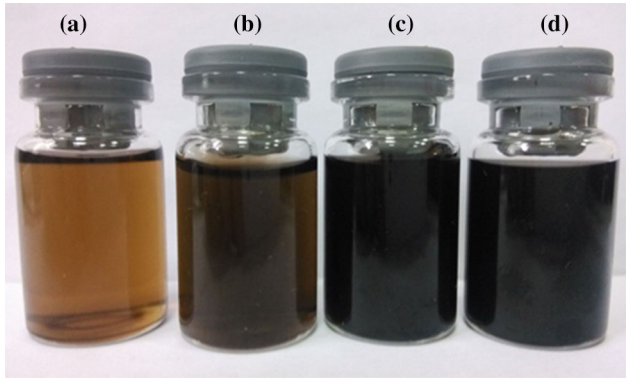

Fig. 1. Photographs of GO dispersions with concentration of 0.1 mg/mL under different conditions. (a) GO dispersions in H_2O/DMF (1:9); GO dispersions in H_2O/DMF (1:9) after reduced by hydrazine monohydrate for 4 h (b), 8 h (c), and 12 h (d) (Color figure online).

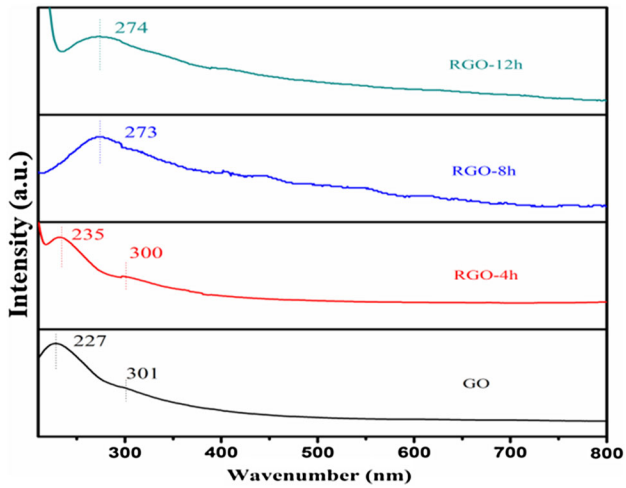

Fig. 2. UV–Vis spectra of GO and RGO with different reduction time in water.

increment of electron density. In addition, it is worth noting that the absorption peak of C=O bonds at ~300 nm disappears gradually with the increasing of the reduction time, which further confirms the graphitization of GO.

XRD Patterns of RGOs

The reduction of GO was also tracked by XRD, as shown in Fig. 3. The initial GO powder shows a sharp diffraction peak centered at $2\theta = 10.46°$, corresponding to a d-spacing of 0.84 nm. When reduced by hydrazine monohydrate, the characteristic diffraction peak (001) of GO decreases gradually with the increasing of the reduction time, and it disappears completely when reduced for 12 h. Meanwhile, a new broad diffraction peak at about 23.5°, corresponding to the (002) planes of graphene, appears and strengthens with the increasing of the reduction time. The XRD result once again confirms

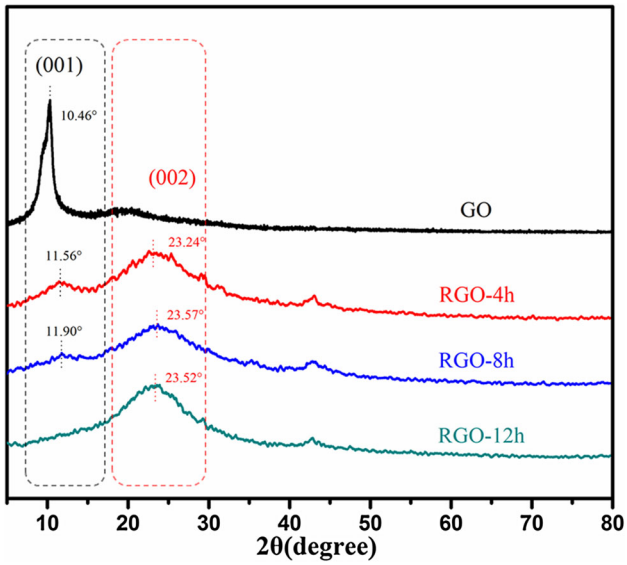

Fig. 3. XRD patterns of GO and RGO with different reduction time.

the removal of oxygen-functional groups from GO sheet and restoration of the graphite structure.[33]

XPS Spectra of GO and RGO

To gain more details about the surface chemical changing of GO during the reduction process, the samples were characterized by x-ray photoelectron spectroscopy (XPS), as shown in Fig. 4. The C1s spectrum of GO could be quantitatively differentiated into four different carbon species [O=C–O, C=O, C–O–C (epoxy/ether), C–OH, and C=C], as shown in Fig. 4a.[34] After the reaction with hydrazine monohydrate at 80°C for 12 h, significant decreases on the intensity of C–O–C peak at 286.79 eV can be observed (Fig. 4b), revealing that epoxy groups on the surface of GO have been effectively consumed by the reductant. As a result, it will further change the interaction between graphene sheets and CuPc molecules.

In order to investigate the effect of RGO on the dielectric properties of RGO/CuPc nanocomposites, the same content of GO (5 wt.%) with different reduction times were mixed with CuPc to form GO/CuPc, RGO-4h/CuPc, RGO-8h/CuPc, and RGO-12h/CuPc nanocomposites, respectively.

Morphology Properties of RGO/CuPc Nanocomposites

SEM was used to study the microstructure of RGO-12h/CuPc (5RGO/CuPc) nanocomposites. As shown in Fig. 5a, the sample of pure CuPc is made up of the porous, fluffy nanospheres, which can be attributed to the self-aggregation of CuPc molecules. For RGO-12h/CuPc, the surface of graphene sheets with coarse morphologies can be observed after introducing CuPc into RGO. Sphere-like nanostructures homogeneously and tightly disperse

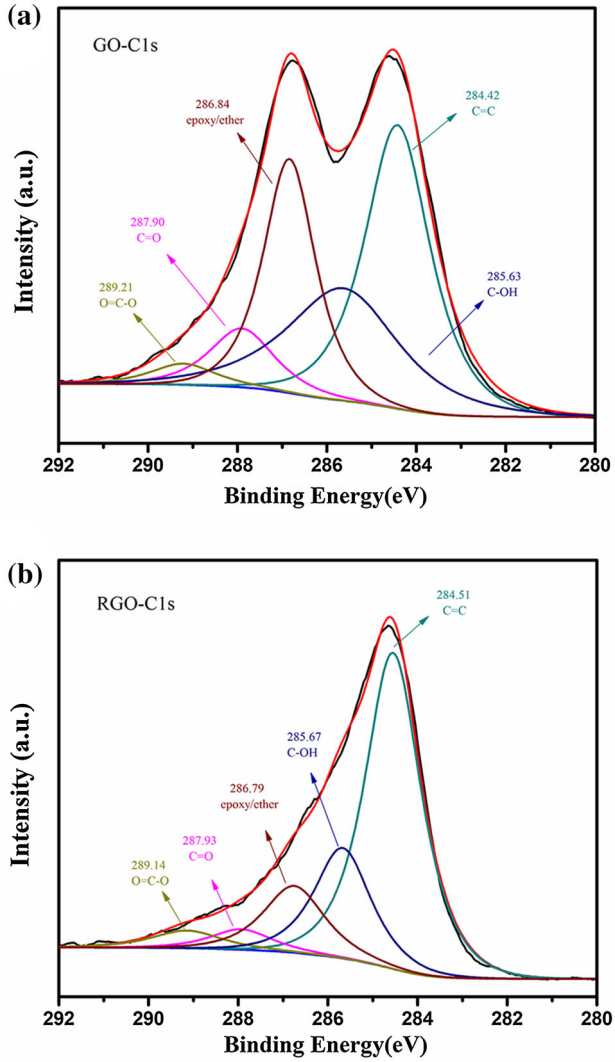

Fig. 4. High resolution C1 s XPS spectra of GO (a) and RGO (b) reduced by hydrazine monohydrate for 12 h.

on the surface of graphene as shown in Fig. 5b. For the system, the formation of hetero-structure demonstrates that RGO/CuPc composites are fabricated successfully via strong intermolecular π–π interaction between graphene sheets and phthalocyanine.

UV–Vis Spectra of RGO/CuPc Nanocomposites

UV–Vis spectrophotometer was employed to trace the effect of RGO on the self-assembly behavior of CuPc, as shown in Fig. 6a. The spectra show characteristic absorption bands at 550–750 nm, corresponding to the Q-band of copper phthalocyanine ring.[35] A slight red-shift of the Q-band with prolonged reduction time can be observed in Fig. 6a. The evolution in UV–Vis spectra is mainly attributed to the enhancement of π–π interaction between CuPc and RGO. As a kind of large 2D planar structure, enhanced π-electron delocalized system of

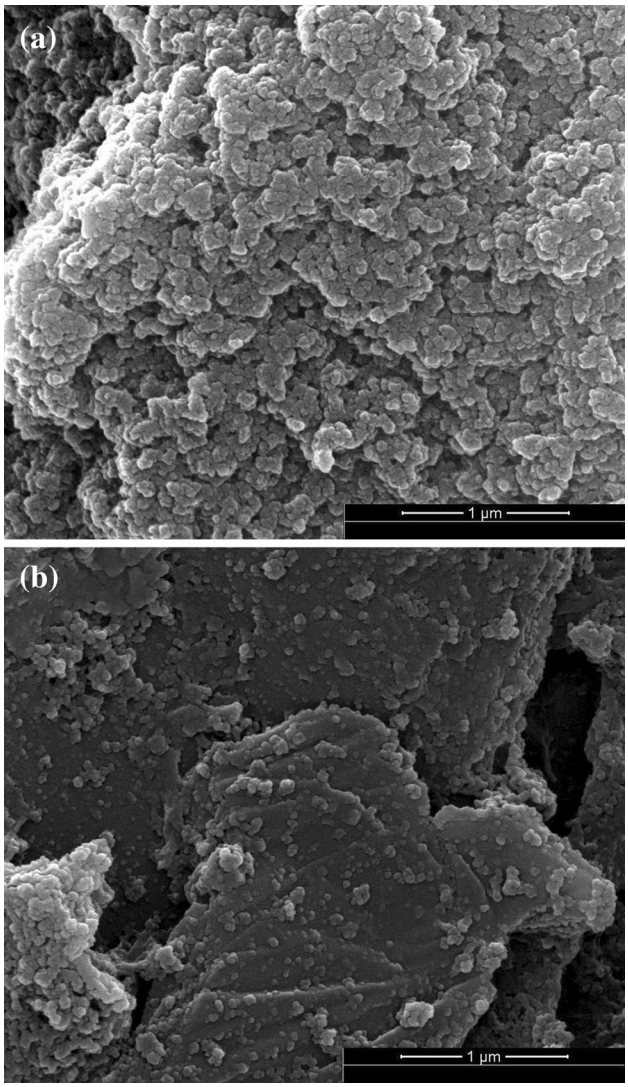

Fig. 5. SEM images of pure CuPc (a) and CuPc nanocomposites with 5 wt.% RGO reduced by hydrazine monohydrate for 12 h (b).

RGO will enhance the interaction with CuPc through π–π interaction, which is beneficial to the fabrication of RGO/CuPc nanocomposites.[30] With the increment of the concentration of RGO, the absorption peak of Q-band exhibits further red-shift from 677.4 nm to 680.2 nm, as shown in Fig. 6b, which also reflects the strong π–π interaction between RGO and CuPc molecule. From the UV–Vis spectra results, it can be concluded that with the increasing of reduction time and concentration of RGO, the π–π interaction between RGO and CuPc molecule gradually strengthens, which will effectively promote the fabrication of RGO/CuPc nanocomposites.

DSC Curves of RGO/CuPc Nanocomposites

DSC measurement was also performed to further study the effect of RGO on the interaction between RGO and CuPc. As shown in Fig. 7a, the GO powder shows a characteristic exothermic peak centered at 192.5°C on the first heating scan, which is mainly attributed to the decomposition of labile oxygen functional groups, yielding CO, CO_2 and water vapour.[36] For CuPc, a distinct and endothermic melting transition (T_m) at 212.8°C can be observed. After self-assembling with 5 wt.% GO sheets, the obtained GO/CuPc nanocomposite shows a new and higher T_m (218.9°C), while the characteristic exothermic peak of GO disappears. Comparing with GO/CuPc, the T_m of the RGO/CuPc nanocomposites decreases gradually with increasing of reduction time, while they are all higher than that of pure CuPc (Fig. 7a). Meanwhile, the T_m of RGO/CuPc shows a tendency to increase with the increasing content of RGO, as shown in Fig. 7b. As reported by Yang et al.,[30] GO is consisted of two parts: oxygen-functional groups and graphitic domain, which is mainly composed of sp^2 carbon. The graphitic domain of GO effectively facilitates interaction with CuPc through π–π stacking. On the other hand, the oxygen-functional groups of GO, especially the carboxyl and epoxy species, tend to act as a ligand that coordinated on the central metal ions of CuPc.[30] The formation of metal–ligand coordination bond strengthens the stability of oxygen-functional groups, which will hinder the breakdown of oxygen functional groups during the reduction process of GO. The synergistic effect of π–π interaction and metal–ligand coordination effectively enhances the T_m of CuPc. After reduction by hydrazine monohydrate, the amount of metal–ligand coordination bond decreases gradually due to the degradation of the oxygen-functional groups (epoxy groups) as shown in Fig. 4. At the same time, the restoration of the π-conjugated network within the graphene and increase of electron density will significantly enhance the π–π interaction between graphene sheets and CuPc molecules (Fig. 6). As a kind of special covalent bond, metal–ligand coordination bond is stronger than the inter-sheet van der Waals attraction (π–π interaction), which will play a leading role in this system. Therefore, as a result of the synergistic effect of the weakening of metal–ligand coordination and enhancing of π–π interaction between RGO and CuPc, the T_m of RGO/CuPc nanocomposites decreases gradually with the increasing of reduction time, while they are all higher than that of pure CuPc. For the RGO/CuPc nanocomposites with different contents of RGO, the increasing content of RGO enhances the π–π interaction between RGO and CuPc effectively, leading to the elevation in the T_m of RGO/CuPc nanocomposites (Fig. 7b).

Dielectric Properties and Alternating Current (AC) Conductivity of RGO/CuPc Nanocomposites

To investigate the effect of RGO on the electrical properties of CuPc, the dielectric constant, dielectric

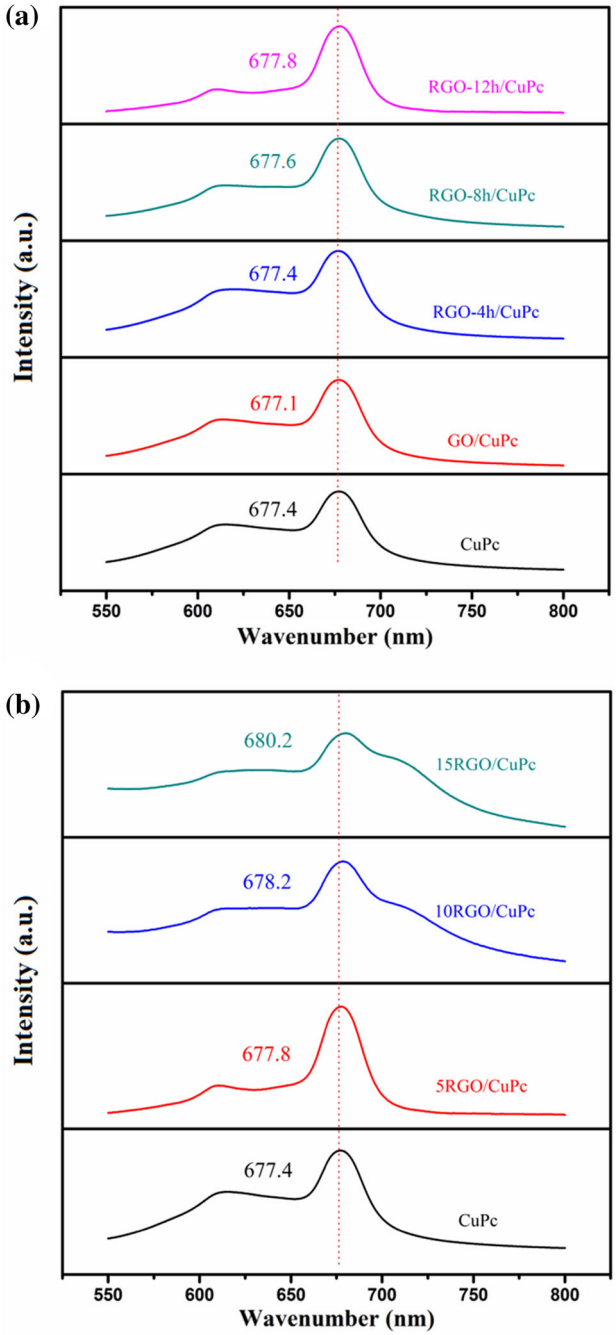

Fig. 6. UV-Vis spectra of CuPc, GO/CuPc, and RGO/CuPc nanocomposites with different reduction time in DMF (a); UV-Vis spectra of CuPc and RGO/CuPc nanocomposites with different content of RGO reduced by hydrazine monohydrate for 12 h in DMF (b).

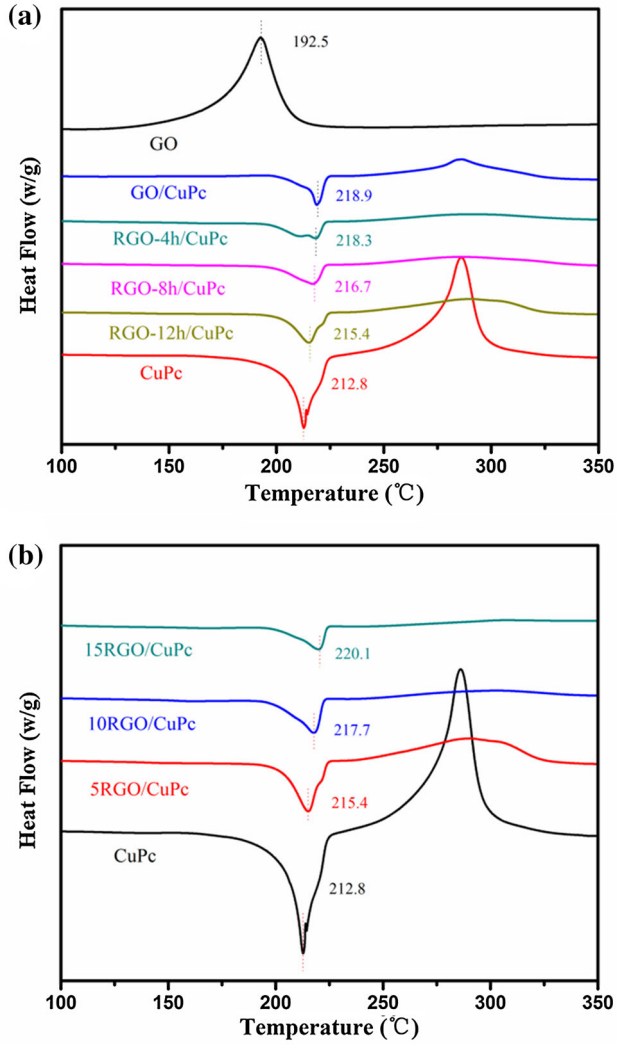

Fig. 7. DSC curves of CuPc, GO/CuPc, and RGO/CuPc nanocomposites with different reduction time (a); DSC curves of CuPc and RGO/CuPc nanocomposites with different content of RGO reduced by hydrazine monohydrate for 12 h (b).

loss, and AC conductivity as a function of applied frequency for the RGO/CuPc nanocomposites were measured at room temperature, and the results are shown in Figs. 8 and 9. It can be clearly seen that the dielectric constant of RGO/CuPc nanocomposites exhibits an obvious dependence on the frequency and increases gradually with increasing of reduction time and the content of RGO, as shown in Figs. 8a and 9a. When the reduction time reaches 12 h, the dielectric constants at 100 Hz and 1 kHz are 9.33 and 6.54, with an increment of 132% and 64% in comparison with that of pure CuPc (4.08 and 3.98), respectively. The substantial improvement in the dielectric properties is attributed to the large specific surface area and high aspect ratio of graphene sheets, which makes it possible to form a microcapacitor structure, isolated by thin dielectric insulating layers of CuPc. Under the applied electric field, the migration and accumulation of charge carriers at interfaces between RGO and CuPc result in an increase in the dielectric properties of the composites at low frequency, known as Maxwell–Wagner–Sillars (MWS) interfacial polarization.[37–39] Owing to the reduction of GO and restoration of the sp^2 carbon sites, more and more charges accumulate at the interface, leading to the increment of the

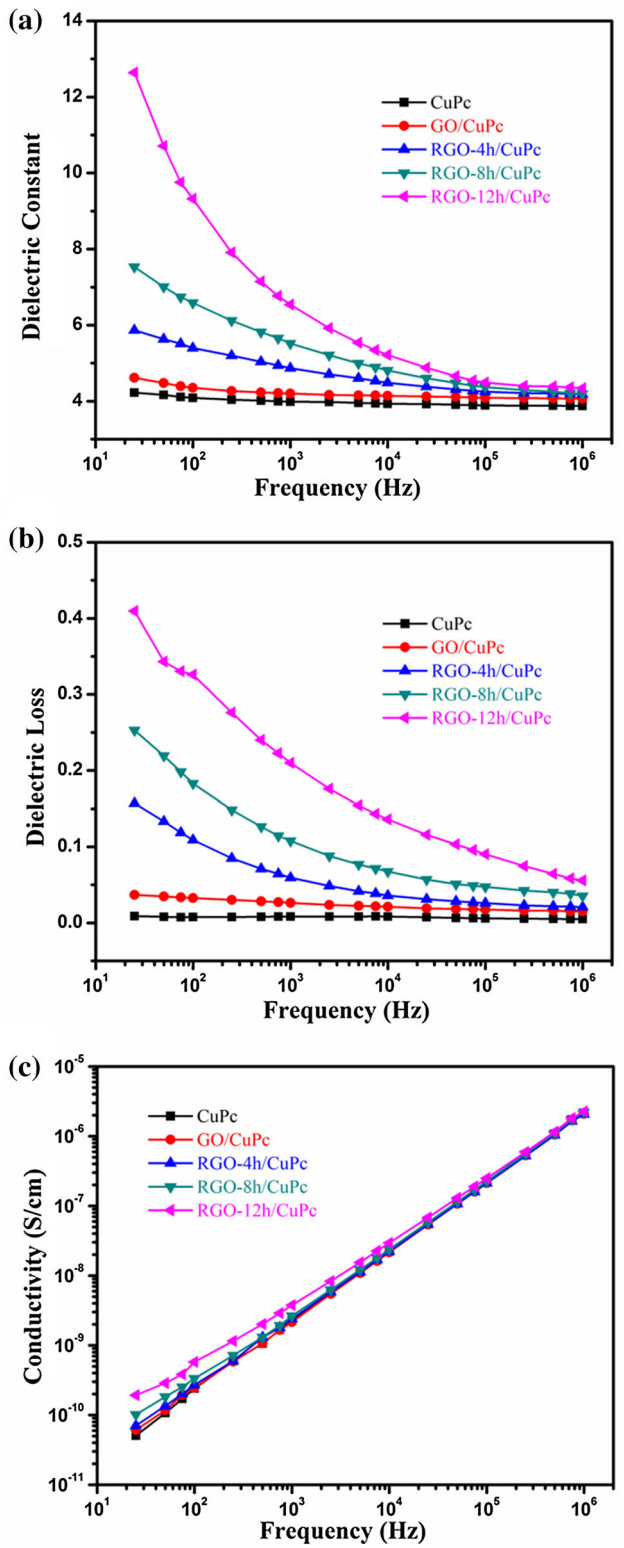

Fig. 8. Dielectric constant (a), dielectric loss (b), and AC conductivity (c) of CuPc, GO/CuPc, and RGO/CuPc nanocomposites with different reduction time.

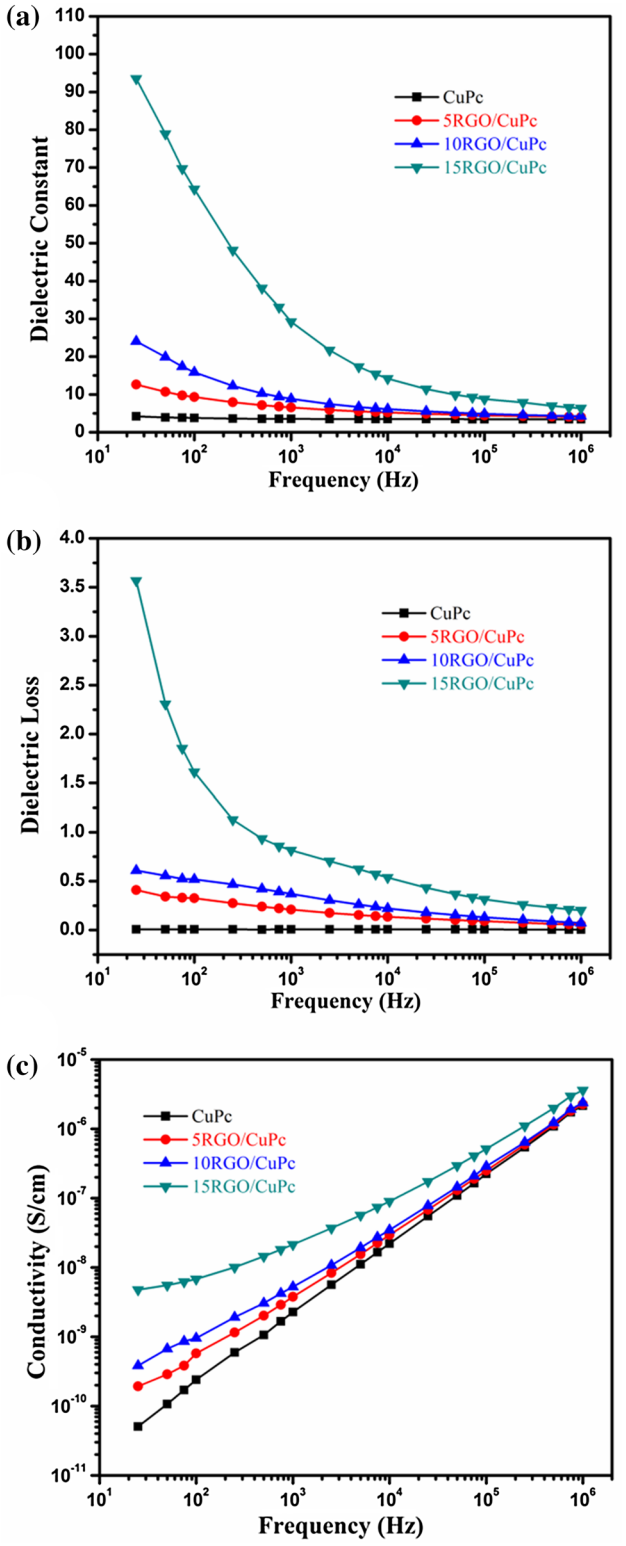

Fig. 9. Dielectric constant (a), dielectric loss (b), and AC conductivity (c) of CuPc and RGO/CuPc nanocomposites with different content of RGO reduced by hydrazine monohydrate for 12 h.

dielectric properties and AC conductivity with increasing of reduction time (Fig. 8). Moreover, similar trends of dielectric loss and AC conductivity can also be observed in Fig. 8b and c, which can also be attributed to interfacial polarization. Under alternating electric field, the lag of induced charges

accumulated at the interface which countered the external applied field result in the dielectric relaxation and transfer the electric energy to heat energy, leading to that the dielectric loss gradually increases and reaches a high value of 0.21 at 1 kHz for RGO-12h/CuPc composites. When the content of RGO increases, the number of the RGO/CuPc microcapacitors increases gradually, leading to the improvement of the dielectric constant of the nanocomposites. As shown in Fig. 9a, the dielectric constant of the nanocomposites with RGO-12h is 9.33 (5 wt.%) and 15.87 (10 wt.%) at 100 Hz, which is 2.3 and 3.9 times larger than that of pure CuPc (4.08), respectively. When the content of RGO is beyond a critical value (percolation threshold), the dielectric constant will increase tremendously, due to formation of the microcapacitor network in the system.[38] As expected, a higher dielectric constant of 64.34 at 100 Hz is obtained for the RGO/CuPc nanocomposites with 15 wt.% RGO, which is 15.8 times than that of pure CuPc. The dielectric loss also exhibits similar increasing trend with increasing the content of RGO and reaches a quite high value as shown in Fig. 9b, which can be ascribed to the formation of the microcapacitor network.

CONCLUSIONS

In summary, reduced graphene oxide/copper phthalocyanine nanocomposites were successfully prepared through a simple and effective two-step method, involving preferential reduction of graphene oxide and followed by self-assembling with CuPc. The results of photographs, UV–Vis, XRD, and XPS confirmed that hydrazine monohydrate removed the oxygen-functional groups especially epoxy groups of GO successfully, which restored the π-conjugated network of graphene. The SEM, UV–Vis spectra and DSC curves indicated that the increasing of the reduction time and the content of RGO can improve the π–π interaction between RGO and CuPc molecule effectively, which promoted the fabrication of RGO/CuPc nanocomposites. Meanwhile, the reduction of GO can also enhance the dielectric properties and AC conductivity of the RGO/CuPc nanocomposites effectively. When the content of RGO reached 15 wt.%, a dielectric constant as high as 64.34 was obtained for the RGO/CuPc nanocomposites, which was about 16 times higher than that of pure CuPc. In conclusion, this type of self-assembly method will provide a facile way to fabricate functional RGO/CuPc composites through π–π interaction and shows great potential of graphene nanocomposites in practical application as organic dielectric materials.

ACKNOWLEDGEMENTS

The financial supports from NSFC (51373028, 51403029), UESTC (A03013023601012), South Wisdom Valley Innovative Research Team Program and Ningbo Major (key) Science and Technology Research Plan (2013B06011) are gratefully acknowledged.

REFERENCES

1. C.X. Guo, M. Wang, T. Chen, X.W. Lou, and C.M. Li, *Adv. Energy Mater.* 1, 736 (2011).
2. X. Huang, X. Qi, F. Boey, and H. Zhang, *Chem. Soc. Rev.* 41, 666 (2012).
3. L. Yan, Y. Zheng, F. Zhao, S. Li, X. Gao, B. Xu, P.S. Weiss, and Y. Zhao, *Chem. Soc. Rev.* 41, 97 (2012).
4. D. Krishnan, F. Kim, J. Luo, R. Cruz-Silva, L.J. Cote, H.D. Jang, and J. Huang, *Nano Today* 7, 137 (2012).
5. R. Raccichini, A. Varzi, S. Passerini, and B. Scrosati, *Nat. Mater.* 14, 271 (2015).
6. K.R. Nemade and S.A. Waghuley, *J. Electron. Mater.* 42, 2857 (2013).
7. C.G. Liu, Z.N. Yu, D. Neff, A. Zhamu, and B.Z. Jang, *Nano Lett.* 10, 4863 (2010).
8. B.F. Machadoab and P. Serp, *Catal. Sci. Technol.* 2, 54 (2012).
9. D. Li, M.B. Muller, S. Gilje, R.B. Kaner, and G.G. Wallace, *Nat. Nanotechnol.* 3, 101 (2008).
10. A.L. Higginbotham, J.R. Lomeda, A.B. Morgan, and J.M. Tour, *ACS Appl. Mater. Interfaces* 1, 2256 (2009).
11. D.D.L. Chung, *J. Mater. Sci.* 51, 554 (2016).
12. A. Lerf, H. He, M. Forster, and J. Klinowski, *J. Phys. Chem. B* 102, 4477 (1998).
13. D.R. Dreyer, S. Park, C.W. Bielawski, and R.S. Ruoff, *Chem. Soc. Rev.* 39, 228 (2010).
14. F.M. Uhl and C. Wilkie, *Polym. Degrad. Stab.* 84, 215 (2004).
15. S. Stankovich, R. Piner, X. Chen, N. Wu, S. Nguyen, and R. Ruoff, *J. Mater. Chem.* 16, 155 (2006).
16. D.A. Dikin, S. Stankovich, E.J. Zimney, R.D. Piner, G.H.B. Dommett, G. Evmenenko, S.T. Nguyen, and R.S. Ruoff, *Nature* 448, 457 (2007).
17. R. Rozada, J.I. Paredes, M.J. López, S. Villar-Rodil, I. Cabria, J.A. Alonso, A. Martínez-Alonso, and J.M.D. Tascón, *Nanoscale* 7, 2374 (2015).
18. J. Gao, C.Y. Liu, L. Miao, X.Y. Wang, and Y. Chen, *J. Electron. Mater.* 45, 1290 (2016).
19. P. Fan, L. Wang, J.T. Yang, F. Chen, and M.Q. Zhong, *Nanotechnology* 23, 365702 (2012).
20. Z.C. Wang, W. Yang, and X.B. Liu, *J. Polym. Res.* 21, 358 (2014).
21. G. Torre, C.G. Claessens, and T. Torres, *Chem. Commun.* 20, 2000 (2007).
22. T.C. Gomes, R.F. de Oliveira, É.M. Lopes, M.S. Klem, D.L.S. Agostini, C.J.L. Constantino, and N. Alves, *J. Mater. Sci.* 50, 2122 (2015).
23. J.A. Gerbec, D. Magana, A. Washington, and G.F. Strouse, *J. Am. Chem. Soc.* 127, 15791 (2005).
24. X.L. Yang, Y.J. Lei, J.C. Zhong, R. Zhao, and X.B. Liu, *J. Appl. Polym. Sci.* 119, 882 (2011).
25. J. Yang, H.L. Tang, Y.Q. Zhan, H. Guo, R. Zhao, and X.B. Liu, *Mater. Lett.* 72, 42 (2012).
26. H. Dai, S.P. Zhang, G.F. Xua, Y.R. Peng, L.S. Gong, X.H. Lia, Y.L. Lia, Y.Y. Lin, and G.N. Chen, *RSC Adv.* 4, 58226 (2014).
27. X. Zhao, R. Zhao, X.L. Yang, J.C. Zhong, and X.B. Liu, *J. Electron. Mater.* 40, 2166 (2011).
28. Z.C. Wang, R.B. Wei, and X.B. Liu, *RSC Adv.* 5, 88306 (2015).
29. G.M. Tsangaris, G.C. Psarras, and N. Kouloumbi, *J. Mater. Sci.* 33, 2027 (1998).
30. J.H. Yang, Y.J. Gao, W. Zhang, P. Tang, J. Tan, A.H. Lu, and D. Ma, *J. Phys. Chem. C* 117, 3785 (2013).
31. T.M. Keller, *J. Polym. Sci. Polym. Chem.* 26, 3199 (1988).
32. J.I. Paredes, S. Villar-Rodil, A. Martínez-Alonso, and J.M.D. Tascón, *Langmuir* 24, 10560 (2008).
33. L. Xu, G. Xiao, C. Chen, R. Li, Y. Mai, G. Sun, and D. Yan, *J. Mater. Chem. A* 3, 7498 (2015).

34. S.J. Park, K.S. Lee, G. Bozoklu, W.W. Cai, S.T. Nguyen, and R.S. Ruoff, *ACS Nano* 2, 572 (2008).
35. Z.C. Wang, W. Yang, J.J. Wei, F.B. Meng, and X.B. Liu, *Mater. Lett.* 123, 6 (2014).
36. M.S. Alhassan, S. Qutubuddin, A.D. Schiraldi, T. Agag, and H. Ishida, *Eur. Polym. J.* 49, 3825 (2013).
37. Z.M. Dang, L. Wang, Y. Yin, Q. Zhang, and Q.Q. Lei, *Adv. Mater.* 19, 852 (2007).
38. F. He, S. Lau, H.L. Chan, and J.T. Fan, *Adv. Mater.* 21, 710 (2009).
39. D.R. Wang, X.M. Zhang, J.W. Zha, J. Zhao, Z.M. Dang, and G.H. Hu, *Polymer* 54, 1916 (2013).